Fluorine Bonding Enhances the Energetics of Protein-Lipid Binding in the Gas Phase

*Lan Liu, Nobar Jalili, Alyson Baergen, Simon Ng, Justin Bailey, Ratmir Derda and John S. Klassen**

Alberta Glycomics Centre and Department of Chemistry, University of Alberta, Edmonton, Alberta, Canada T6G 2G2

*Email: john.klassen@ualberta.ca

Abstract

This paper reports on the first experimental study of the intrinsic energetics of non-covalent fluorine bonding in a protein-ligand complex. Arrhenius parameters were measured for the dissociation of gaseous deprotonated ions of complexes of bovine β-lactoglobulin (Lg), a model lipid-binding protein, and four fluorinated analogs of stearic acid (SA), which contained (X =) 13, 15, 17 or 21 fluorine atoms. In all cases, the activation energies (E_a) measured for the loss of neutral XF-SA from the $(Lg + XF\text{-}SA)^{7-}$ ions are larger than for SA. From the kinetic data the average contribution of each $>CF_2$ group to E_a was found to be ~1.1 kcal mol^{-1}, which is larger than the ~0.8 kcal mol^{-1} value reported for $>CH_2$ groups. Based on these results it is proposed that fluorocarbon-protein interactions are intrinsically more stable than the corresponding hydrocarbon interactions.

Introduction

The incorporation of fluorine substituents into pharmacologically active compounds is a common strategy used to improve their bioavailability, metabolic stability, and distribution [1-5]. Fluorination of drug molecules can also affect their non-covalent interactions with other molecules, notably proteins [6-10].Understanding the molecular basis of how fluorination influences the affinity and selectivity of protein-ligand interactions is attracting increased attention [8,11,12].Theoretical and experimental studies carried out on non-covalent complexes involving small fluorine-containing molecules indicate that fluorine can alter non-covalent binding either directly, through intermolecular interactions, or indirectly, through the modulation of the polarity of other groups that engage in intermolecular interactions [13-21].At present, the influence of fluorine bonding on the stability of protein-ligand complexes is unclear. A survey of reported crystal structures for proteins bound to fluorinated ligands revealed a large number of interactions between the carbon-fluorine (C-F) unit and polar and non-polar hydrogens [22].According to theoretical calculations performed on model systems, such interactions, although relatively weak, are expected to be energetically more significant than similar interactions involving hydrocarbons [22].However, from a detailed investigation into the binding of alkyl- and fluoroalkyl-substituted benzenesulfonamide ligands to human carbonic anhydrase II (HCA II),it was recently concluded that differences in the binding thermodynamics reflect differences in hydrophobic surface area and not differences in the strength of the intermolecular interactions [23].Here, we report on the first quantitative investigation of the intrinsic energetics (free from solvent effects) of fluorine bonding in a protein-ligand complex. The results of this study provide unambiguous evidence that fluorination of ligand alkyl chains enhances their intermolecular interactions with proteins.

Bovine β-lactoglobulin (Lg), which possesses a large hydrophobic cavity [24,25], and its interactions with four fluorinated analogs of stearic acid (XF-SA) containing X = 13, 15, 17 or 21 fluorine atoms(Figure S1, Supplementary Information) served as model systems for this study. The Arrhenius parameters for the loss of neutral ligand from the gaseous $(Lg + XF\text{-}SA)^{7-}$ ions were measured using Fourier-transform ion cyclotron resonance mass spectrometry and the blackbody infrared radiative dissociation (BIRD)technique [26,27].The nature of the intermolecular interactions in the gaseous $(Lg + XF\text{-}SA)^{7-}$ ions were investigated using molecular dynamics (MD) simulations.

Deprotonated gas-phase ions of the (Lg + XF-SA) complexes were readily detected by ESI-MS performed in negative ion mode on aqueous ammonium acetate (10 mM) solutions containing Lg and one of the water-insoluble XF-SA ligands(initially dissolved in methanol) at 25 °C and pH 8.5 (Figure S2, Supplementary Information). Imidazole (10 mM), which is known to minimize the extent of in-source (gas-phase) dissociation, was also added to each solution [28,29].At pH >8, Lg is known to exist predominantly as a monomer and to adopt an "open" structure that allows ligand access to the hydrophobic cavity [24,25].Time-resolved BIRD measurements were performed on the $(Lg + XF\text{-}SA)^{7-}$ ions at temperatures ranging from 37 to 77°C. As illustrated in Figure S3, Supplementary Information, BIRD of the $(Lg + X\text{-}FSA)^{7-}$ ions proceeds exclusively by the loss of neutral XF-SA, eq 1:

$$(Lg + XF\text{-}SA)^{7-} \rightarrow Lg^{7-} + XF\text{-}SA \quad (1)$$

Natural log plots of the normalized abundance (Ab/Ab_{total}) of the $(Lg + XF\text{-}SA)^{7-}$ ions versus reaction time are shown in Figure S4, Supplementary Information, for each ligand investigated. In all cases, the kinetic plots exhibit non-linear behavior that can be described by a double exponential function, indicating the presence of two distinct structures. These findings are

consistent with those reported recently for the dissociation of the deprotonated ions of Lg complexes with saturated, unsaturated and branched fatty acids (FA) [30,31].In these earlier works, the two non-interconverting structures identified in the gas phase were designated as the *fast* and *slow*(dissociating) components, i.e., $(Lg + FA)_f^{n-}$ and $(Lg + FA)_s^{n-}$ ions, respectively. According to the results of MD simulations, the acyl chain remains buried in the hydrophobic cavity in both the *fast* and *slow* structures, the main structural difference being the position of the flexible EF loop of Lg [31]. In the $(Lg + FA)_f^{7-}$ions, the loop is in an "open" position, such that the FA is stabilized predominantly by protein-lipid interactions. Available experimental data suggest that the *fast* component resembles the native structure in solution[30,31].In the $(Lg + FA)_s^{7-}$ ions, the loop is in a "closed" position and H-bonds between the FA carboxyl group and Lg also contribute to the stability of the complex. Given the structural similarities of the FAs considered here and those investigated previously[30,31], it is reasonable to expect that similar structural differences are responsible for the double exponential kinetics observed for the $(Lg + XF\text{-}SA)^{7-}$ ions.

Arrhenius plots (Figure 1) were constructed from the rate constants measured for both the $(Lg + XF\text{-}SA)_f^{7-}$and $(Lg + XF\text{-}SA)_s^{7-}$ ions, i.e., k_f and k_s, respectively, and the corresponding Arrhenius parameters (E_a and A) are listed in Table 1. For comparison purposes, the Arrhenius plots and parameters for the dissociation of the $(Lg + SA)_f^{7-}$ and $(Lg + SA)_s^{7-}$ions are also included [31]. Inspection ofthe Arrhenius parameters reveals that fluorination of the acyl chain of SA results in a significant increase in E_a values for both the *fast* and the *slow* components. A plot of E_a versus number of fluorine substitutions is shown in Figure 2. In the case of the *fast* component, E_a increases linearly with the number of fluorines, with each fluorine contributing an additional ~0.15 kcal mol^{-1}. The average contribution of each $>CF_2$ to E_a value is ~1.12 ± 0.01

kcal mol^{-1} for the *fast* component, which is 0.30 kcal mol^{-1} higher than the value (0.82± 0.04 kcal mol^{-1}) reported for $>CH_2$ groups [31].The linear increase in E_a with number of fluorine substitutions suggests that the Lg cavity presents a relatively homogeneous environment to the $>CF_2$ groups. The average energetic contribution of $-CF_3$ to the E_a of the *fast* component (estimated as the difference between the measured $E_a$value and the combined energetic contributions of the $>CF_2$ and $>CH_2$ groups) is 1.85 ± 0.15 kcal mol^{-1}, compared to 1.29 kcal mol^{-1} for the $-CH_3$ group [30].Taken together, these results provide irrefutable evidence that Lg bonding to fluoroalkyl chains is energetically more favourable than to the corresponding alkyl chains in the gas phase.

No correlation between E_a and the number of fluorines in the XF-SA ligands is evident for the *slow* component. This finding is not unexpected and is consistent with results obtained previously for the *slow* components of $(Lg + FA)^{n-}$ions composed of saturated FAs of different lengths or FAs with different degrees of unsaturation [30].As described above and elsewhere [30,31],the *slow* component is believed to be stabilized by both protein-lipid interactions and hydrogen bonding involving the FA carboxyl group and that changes in protein-lipid binding resulted in changes to the nature of the hydrogen bond(s). Consequently, the present results suggest that the degree of fluorination alters the nature of the interactions between the carboxyl group and Lg in the $(Lg + XF\text{-}SA)_s^{7-}$ ions.

Shang and coworkers have calculated energies for C-F interactions representative of those found in protein-ligand complexes [11]. Comparison of the average energetic contribution that C-F makes to the E_a for the $(Lg + XF\text{-}SA)_f^{7-}$ions with the calculated energies reveals that the experimental value most closely resembles those found for C-F interactions with polar hydrogens. For example, at the MP2 level of theory and using the 6-311++G(d,p) basis set, an

interaction energy of 1.60 kcal mol^{-1} was found [11].Other neutral interactions suggested to be important in protein-ligand binding, such those involving nonpolar hydrogens or amide carbonyls (so-called orthogonal multipolar interactions) are too weak to account for the experimental results[11].

To probe the nature of the stabilizing intermolecular interactions in more detail, MD simulations were performed on the $(Lg + 13F\text{-}SA)^{7-}$ and $(Lg + 21F\text{-}SA)^{7-}$ ions using the Amber 12SB force field for Lg and the general Amber force field for the ligands [32,33].Analysis of the trajectories shows that, for a given charge configuration, close to half the fluorine atoms form interactions with nearby polar hydrogen atoms associated with amino acid side chains and backbone amides (Figure S5, Supplementary Information). However, these interactions are transient (a given fluorine bond exists for only 10-50% of the trajectory) and individual residues can interact, in an alternating fashion, with multiple fluorine atoms (Figure S6, Supplementary Information). Although the individual fluorine bonds are apparently weak, their combined effects would, nevertheless, be expected to enhance the kinetic stabilities of the $(Lg + XF\text{-}SA)^{7-}$ ions over those of the corresponding $(Lg + SA)^{7-}$ions. The results of the MD simulations also suggest that the degree of fluorination of SA influences the nature of the hydrogen bonds involving the carboxyl group. This finding provides a qualitative explanation for the absence of correlation degree of fluorination on the E_a values for the$(Lg + XF\text{-}SA)_s^{7-}$ions.

The present results clearly demonstrate that fluorocarbon binding within the hydrophobic cavity of Lg is energetically preferred to hydrocarbon binding. Given that there is nothing remarkable about the residues that make up the Lgcavity, 12 aliphatic residues (Leu58, Val41, Val43, Leu46, Leu54, Ile56, Leu58, Ile71, Leu87, Val92 and Leu103) and one aromatic residue (Phe105), it is reasonable to conclude that fluorocarbon binding inside hydrophobic protein

cavities will generally be energetically more favourable than hydrocarbon binding and, in the absence of differential solvent effects, will lead to enhanced binding in aqueous solution. If that is indeed the case, then the present findings would seem to argue for a refinement of the conclusions drawn recently by Whitesides and coworkers regarding the origin of the thermodynamic differences in binding of alkyl and fluoroalkyl groups to HCA II [23].Fluorination was found to enhance both the enthalpy and entropy of ligand binding to the protein. The authors concluded that these changes arose primarily from differences in the solvent accessible surface area of hydrocarbon and fluorocarbon moieties and not from differences in intermolecular interaction energies. While it is possible that in the case of HCA II the interactions with alkyl and fluoroalkyl chains are energetically similar, it is more likely that the thermodynamic differences do reflect, at least in part, a greater intrinsic stability of the fluorinated ligands.

In summary, the intrinsic energetics of non-covalent fluorine bonding in a protein-ligand complex were measured for the first time. Fluorination of SA was found to increase the dissociation E_a for ligand loss from complexes with Lg in the gas phase. The average energetic contribution of $>CF_2$ groups to $E_a$is measurably larger than the value reported previously for $>CH_2$ groups and relatively insensitive to position on the alkyl chain, suggesting that the Lg cavity presents a relatively homogeneous solvation environment to the fluoroalkyl chains. According to the results of MD simulations, fluorine bonding to polar hydrogens is primarily responsible for the stabilizing effect of fluorination. Future efforts will investigate the stabilities of other protein-ligand complexes in the gas phase, including those of HCA II, with the goal of more generally establishing the influence fluorine bonding on the thermodynamics of protein-ligand interactions.

Acknowledgements

The authors are grateful for financial support provided by the Natural Sciences and Engineering Research Council of Canada and the Alberta Glycomics Centre.

References

1. Banks, R. E.; Smart, B. E.; Tatlow, J. C.:Organofluorine Chemistry: Principles and Commercial Applications, Plenum Press, New York, (1994).

2. Clader, J. W.: The Discovery of Ezetimibe: a View from Outside the Receptor.*J. Med. Chem*. **47**, 1-9 (2004).

3. Hugel, H. M.; Jackson, N.:Special Feature Organo-Fluorine Chemical Science, *Appl. Sci.* **2**, 558-565 (2012).

4. Gunduz, M.; Argikar, U. A.; Kamel, A.; Colizza, K.; Bushee, J.; Cirello, A.; Lombardo, F.; Harriman, S.: Oxidative *ipso* Substitution of 2,4-Difluoro-benzylphthalazines: Identification of a Rare Stable Quinone Methide and Subsequent GSH Conjugate,*DrugMetab. Dispos*. **40**, 2074-2080(2012).

5. Vasdev, N.; Dorff, P. N.; O'Neil, J. P.; Chin, F. T.; Hanrahan, S.; Van Brocklin, H. F.: Metabolic Stability of 6,7-dialkoxy-4-(2-,3-and 4-[^{18}F]fluoroanilino)quinazolines, Potential EGFR Imaging Probes, *Bioorg. Med Chem*.**19**, 2959-2965 (2011).

6. Böhm, H.; Banner, D.; Bendels, S.; Kansy, M.; Kuhn, B.; Müller, K.; Obst-Sander, U.; Stahl, M.: Fluorine in Medicinal Chemistry. *ChemBioChem***5**, 637-643 (2004).

7. Kim, C.; Chang, J. S.; Doyon, J. B.; Baird, T. T. Jr.; Fierke, C. A.; Jain, A.; Christianson, D. W.:Contribution of Fluorine to Protein-Ligand Affinity in the Binding of Fluoroaromatic Inhibitors to Carbonic Anhydrase II.*J. Am. Chem. Soc.***122**, 12125-12134(2000).

8. Rendine, S.; Pieraccini, S.; Forni, A.; Sironi, M.:Halogen Bonding in Ligand–Receptor Systems in the Framework of Classical force fields. *Phys. Chem. Chem. Phys*. **13**, 19508-19516 (2011).

9. Benitex, Y.; Baranger, A.: M.Control of the Stability of a Protein-RNA Complex by the Position of Fluorine in a Base Analogue. *J. Am. Chem. Soc.***133**,3687-3689 (2011).

10. Lee, Y.; Zeng, H.; Ruedisser, S.; Gossert, A. D.; Hilty, C.:Nuclear Magnetic Resonance of Hyperpolarized Fluorine for Characterization of Protein-Ligand Interactions.*J. Am. Chem. Soc.***134**, 17448-17451(2012).

11. Zhou, P.; Zou, J.; Tian, F.; Shang, Z.:Fluorine Bonding s How Does It Work In Protein-Ligand Interactions. *J. Chem. Inf. Model*. **49**, 2344-2355 (2009).

12. Kuhn, B.; Kollman, P. A.:A Ligand That Is Predicted to Bind Better to Avidin than Biotin: Insights from Computational Fluorine Scanning.*J. Am. Chem. Soc*. **122,**3909-3916 (2000).

13. Kawahara, S.; Tsuzuki, S.; Uchimaru, T.:Theoretical Study of the C-F/πInteraction: Attractive Interaction between Fluorinated Alkane and an Electron-Deficient π–System. *J. Phys. Chem. A.* **108**, 6744-6749 (2004).

14. Riley, K. E.; Merz, K. M.: Effects of Fluorine Substitution on the Edge-to-Face Interaction of the Benzene Dimer.*J. Phys. Chem. B.***109**,17752-17756 (2005).

15. Chopra, D.; Nagarajan, K.; Row, T. N. G. Analysis of Weak Interactions Involving Organic Fluorine: InsightsfromPacking Features in Substituted 4-keto-tetrahydroindoles, *J. Mol. Struct*. **888**, 70-83(2008).

16. Iwaoka, M.; Komatsu, H.; Katsuda, T.; Tomoda, S.:Quantitative Evaluation of Weak Nonbonded Se···FInteractions and Their Remarkable Nature as Orbital Interactions.*J. Am. Chem. Soc.* **124**, 1902-1909 (2002).

17. Matta, C. F.; Castillo, N.; Boyd, R. J.: Characterization of a Closed-Shell Fluorine-Fluorine Bonding Interaction in AromaticCompounds on the Basis of the Electron Density. *J. Phys. Chem. A.* **109**, 3669-3681(2005).

18. Lee, S.; Mallik, A. B.; Fredrickson, D. C.:Dipolar-Dipolar Interactions and the Crystal Packing of Nitriles, Ketones, Aldehydes, and C(sp^2)-F Groups. *Cryst. Growth Des*.**4,** 279-290(2004).

19. Olsen, J. A.; Banner, D. W.; Seiler, P.; Sander, U. O.; D'Arcy, A.;Stihle, M.; Müller, K.; Diederich, F.:A Fluorine Scan of Thrombin Inhibitors to Mapthe Fluorophilicity/Fluorophobicity of an EnzymeActive Site: Evidence for C-F···C=OInteractions.*Angew. Chem. Int.Ed.***42,** 2507-2511 (2003).

20. Plenio, H.: The Coordination Chemistry of Fluorine in Fluorocarbons. *ChemBioChem.***5**, 650-655 (2004).

21. Bettinger, H. F.:How Good is Fluorine as a Hydrogen-Bond Acceptor in Fluorinated Single-Walled Carbon Nanotubes?*ChemPhysChem*.**6**,1169-1174 (2005).

22. Müller, K.;Faeh, C.; Diederich, F. Fluorine in Pharmaceuticals: Looking Beyond Intuition.*Scienc***317***,* 1881-1886 (2007).

23. Mecinović, J.; Snyder, P. W.; MIRICA, K. A; Bai, S.; Mack, E. T.; Kwant, R. L.; Moustakas, D. T.; Héroux, A.; Whitesides, G. M.:Fluoroalkyl and Alkyl Chains Have Similar Hydrophobicities in Binding to the "Hydrophobic Wall" of Carbonic Anhydrase. *J. Am. Chem. Soc.***133**,14017-14026 (2011).

24. Kontopidis, G.; Holt, C.; Sawyer, L.:Beta-Lactoglobulin: Binding Properties, Structure, and Function.*J. Dairy Sci*. **87,** 785-796 (2004).

25. Qin, B.Y.; Bewley, M.C.; Creamer, L.K.; Baker, H.M.; Baker, E.N.; Jameson, G.B.: Structural Basis of the Tanford Transition of Bovine Beta-Lactoglobulin,*Biochem.* **37**, 14014-14023 (1998).

26. Dunbar, R.C., McMahon, T.B.: Activation of Unimolecular Reactions by Ambient Blackbody Radiation. *Science***279**, 194-197 (1998).

27. Price, W.D.;Schnier, P.D.; Jockusch, R.A.; Strittmatter, E.R.; Williams, E.R.: Unimolecular Reactions Kinetics in the High-Pressure Limit Without Collisions.*J. Am. Chem. Soc.**118***, 10640-10644 (1996).

28. Sun, J.; Kitova, E.N.;Klassen, J.S.: Method for Stabilizing Protein-Ligand Complexes in Nnanoelectrospray Ionization Mass Spectrometry. *Anal. Chem*. **79**, 416-425 (2007).

29. Bagal, D.; Kitova, E.N.; Liu, L.; El-Haweit, A.; Schnier, P. D.;Klassen, J.S.:Gas Phase Stabilization of Noncovalent Protein Complexes Formed by Electrospray Ionization. *Anal. Chem*. **81**, 7801-7806 (2009).

30. Liu, L.; Michelsen, K.; Kitova, E. N.; Schnier, P. D.;Klassen, J. S.: Energetics of Lipid Binding in a Hydrophobic Protein Cavity. *J. Am. Chem. Soc.* **134**, 3054-3060 (2012).

31. Liu, L.; Bagal, D.;Kitova, E. N.; Schnier, P. D.; Klassen, J. S.: Hydrophobic Protein-Ligand Interactions Preserved in the Gas Phase. *J. Am. Chem. Soc.* **131**, 15980-15981(2009).

32. Case, D. A.; Darden, T. A.; Cheatham, T. E.; Simmerling, C. L.; Wang, J.; Duke, R. E.; Luo, R.; Walker, R. C.; Zhang, W.; Merz, K. M.; Roberts, B.; Hayik, S.; Roitberg, A.; Seabra, G.; Swails, J.; Goetz, A. W.; Kolossváry, I.; Wong, K. F.; Paesani, F.; Vanicek, J.; Wolf, R. M.; Liu, J.; Wu, X.; Brozell, S. R.; Steinbrecher, T.; Gohlke, H.; Cai, Q.; Ye, X.; Wang, J.; Hsieh, M. -J.; Cui, G.; Roe D. R.; Mathews D. H.; Seetin M. G.; Salomon-Ferrer, R.; Sagui, C.; Babin V.; Luchko, T.; Gusarov, S.; Kovalenko A.; Kollman, P. A.:AMBER 12. University of California: San Francisco (2012).

33. Wang, J.; Wolf, R. M.; Caldwell, J. W.; Kollman, P. A.; Case, D. A.:Development and Testing of a General Amber Force Field. *J. Comput. Chem.* **25**, 1157-1174 (2004).

Table 1. Arrhenius parameters (E_a, A) determined for the loss of neutral ligand from the gaseous, deprotonated $(Lg + XF\text{-}SA)_f^{7-}$ and $(Lg + XF\text{-}SA)_s^{7-}$ ions.[a]

Ligand	E_a(kcal mol^{-1})	A(s^{-1})
	Fast	
SA	18.0 ± 0.6 [b]	$10^{11.3\pm0.4}$ [b]
13F-SA	20.1 ± 0.2	$10^{12.4\pm0.1}$
15F-SA	20.5 ± 0.3	$10^{12.8\pm0.4}$
17F-SA	20.8 ± 0.4	$10^{13.0\pm0.2}$
21F-SA	21.1 ± 0.5	$10^{13.1\pm0.3}$
	Slow	
SA	21.5 ± 0.5 [b]	$10^{12.7\pm0.3}$ [b]
13F-SA	27.9 ± 1.1	$10^{16.4\pm0.7}$
15F-SA	26.3 ± 1.7	$10^{15.4\pm2.2}$
17F-SA	24.7 ± 1.1	$10^{14.4\pm0.8}$
21F-SA	25.6 ± 1.5	$10^{14.9\pm2.1}$

a. The reported errors are one standard deviation. b. Values taken from reference [31].

Figure captions

Figure 1. Arrhenius plots for the loss of neutral ligand from the $(Lg+XF\text{-}SA)_f^{7-}$ (solid circles) and $(Lg+XF\text{-}SA)_s^{7-}$ ions (open circles) whereX = 0(●), 13 (●), 15 (●), 17 (●)and 21 (●).

Figure 2. Plot of E_a for dissociation of the fast(●) and slow(●) components of the $(Lg+XF\text{-}SA)^{7-}$ ions versus X, the number of fluorine substitutions.

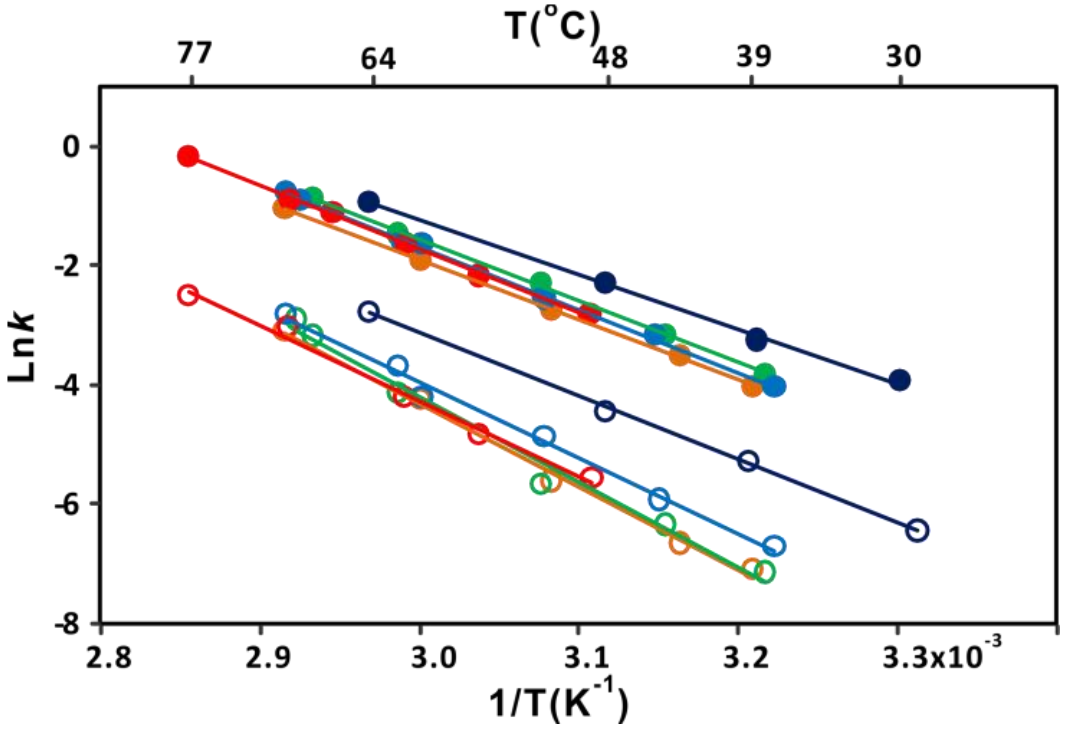

Figure 1

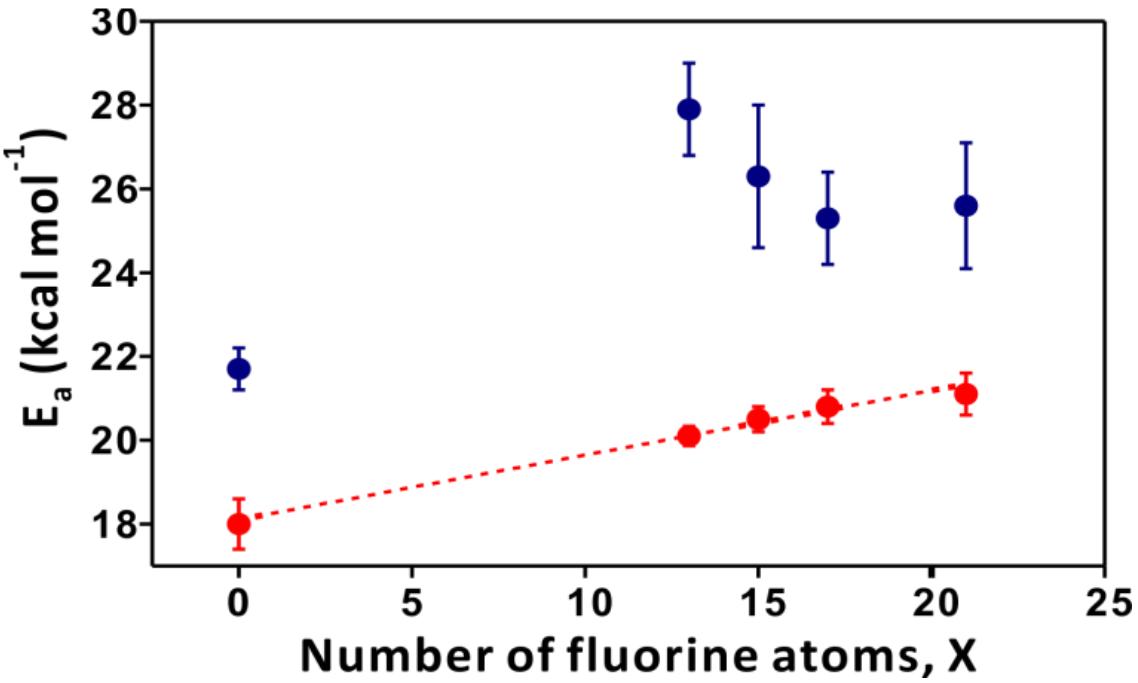
30
28
26
24
22
20
18
E_a (kcal mol^{-1})
0
5
10
15
20
25
Number of fluorine atoms, X

Figure 2

Graphical abstract

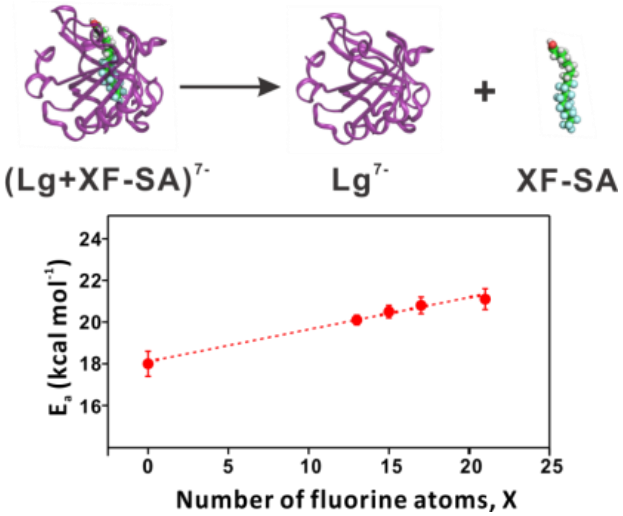

Supplementary information for:

Fluorine Bonding Enhances the Energetics of Protein-Lipid Binding in the Gas Phase

Lan Liu, Nobar Jalili, Alyson Baergen, Simon Ng, Justin Bailey, Ratmir Derda and John S. Klassen

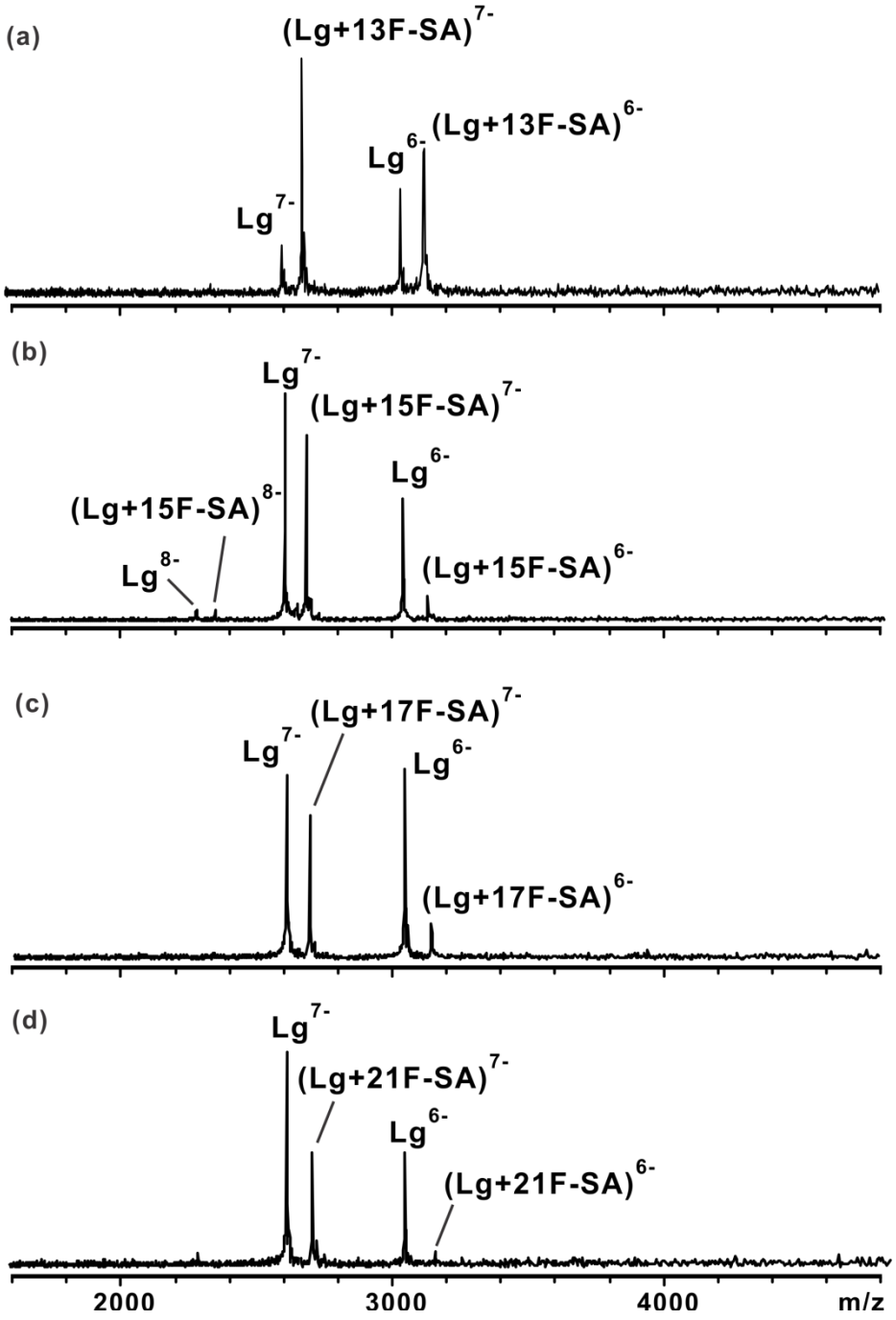

Figure S1. ESI mass spectra acquired for aqueous solutions (pH 8.5, 25 °C) of Lg (15 μM) and (a) 13F-SA, (b) 15F-SA, (c) 17F-SA, and (d) 21F-SA. Each solution contained 10 mM ammonium acetate and 10 mM imidazole.

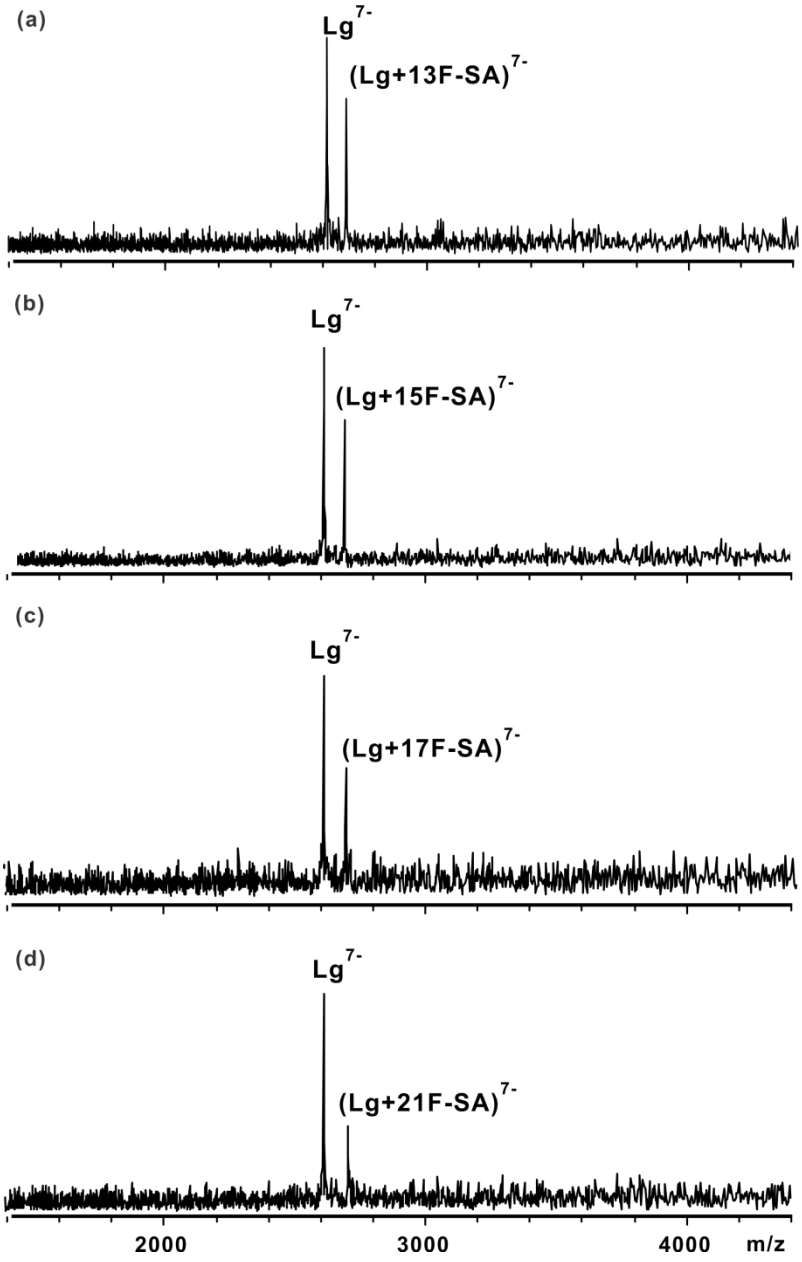

Figure S2. Illustrative BIRD mass spectra measured for (a) $(Lg + 13F\text{-}SA)^{7-}$ at a reaction temperature of 61 °C and a reaction time of 30 s; (b) $(Lg + 15F\text{-}SA)^{7-}$ at 52 °C and 58 s; (c) $(Lg + 17F\text{-}SA)^{7-}$ at 60 °C and 52 s; and (d) $(Lg + 21F\text{-}SA)^{7-}$ at 69 °C and 10 s.

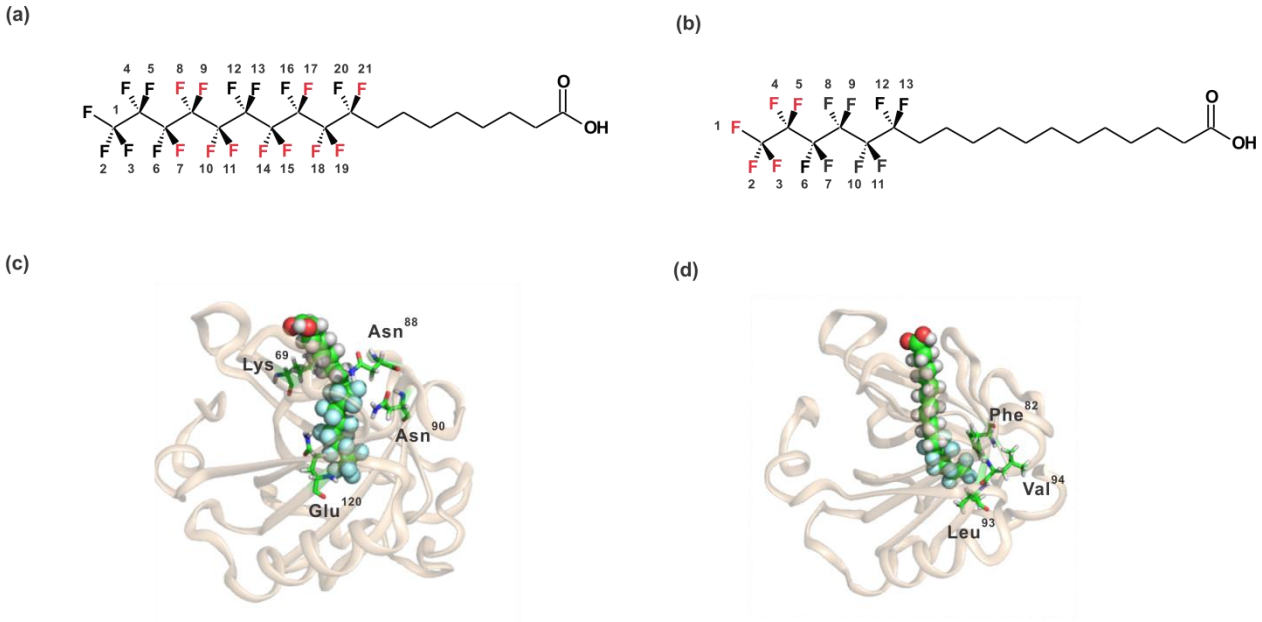

Figure S3. Labelled in red are the fluorine atoms in (a) 21F-SA and (b) 13F-SA that are involved in intermolecular interactions with polar hydrogen in Lg, as determined from MD simulations performed on the $(Lg + 21F\text{-}SA)^{7-}$ ion and$(Lg + 13F\text{-}SA)^{7-}$, respectively. The Lg residues that were deprotonated for this simulation were Asp^{11}, Asp^{28}, Asp^{85}, Asp^{129}, Glu^{51}, Glu^{112}, Glu^{127}. (c) Representative structure of the $(Lg + 21F\text{-}SA)^{7-}$ ion, obtained from the MD simulations, showing the amino acid residues involved in fluorine bonding. The corresponding distance and angle distributions for these interactions are shown in Figure S4. (d) Representative structure of the $(Lg + 13F\text{-}SA)^{7-}$ ion, obtained from the MD simulations, showing the amino acid residues involved in fluorine bonding. The corresponding distance and angle distributions for these interactions are shown in Figure S5.

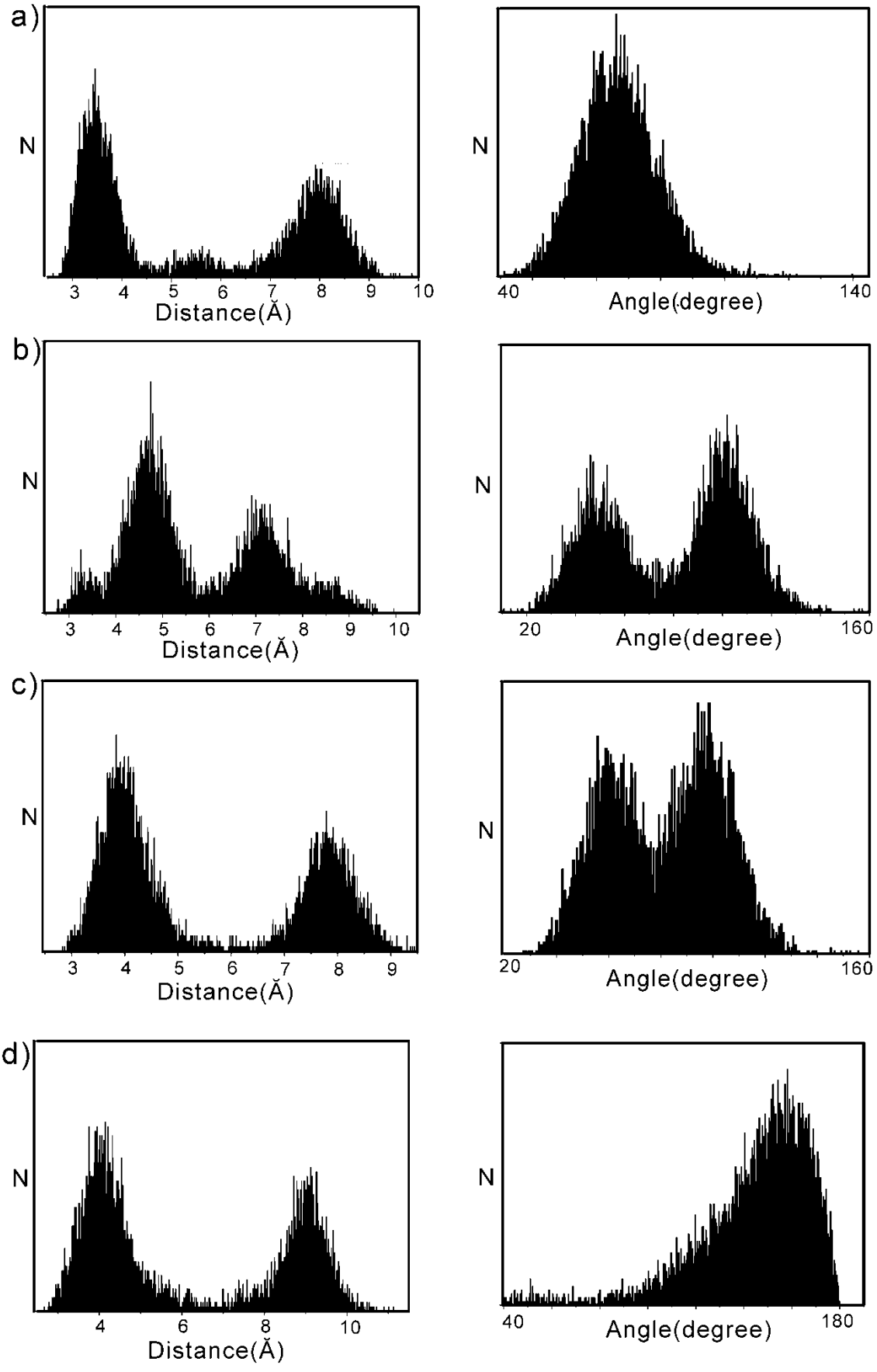
a)
N
3 4 5 6 7 8 9 10
Distance(Ă)
N
40
Angle(degree)
140
b)
N
3 4 5 6 7 8 9 10
Distance(Ă)
N
20
Angle(degree)
160
c)
N
3 4 5 6 7 8 9
Distance(Ă)
N
20
Angle(degree)
160
d)
N
4 6 8 10
Distance(Ă)
N
40
Angle(degree)
180

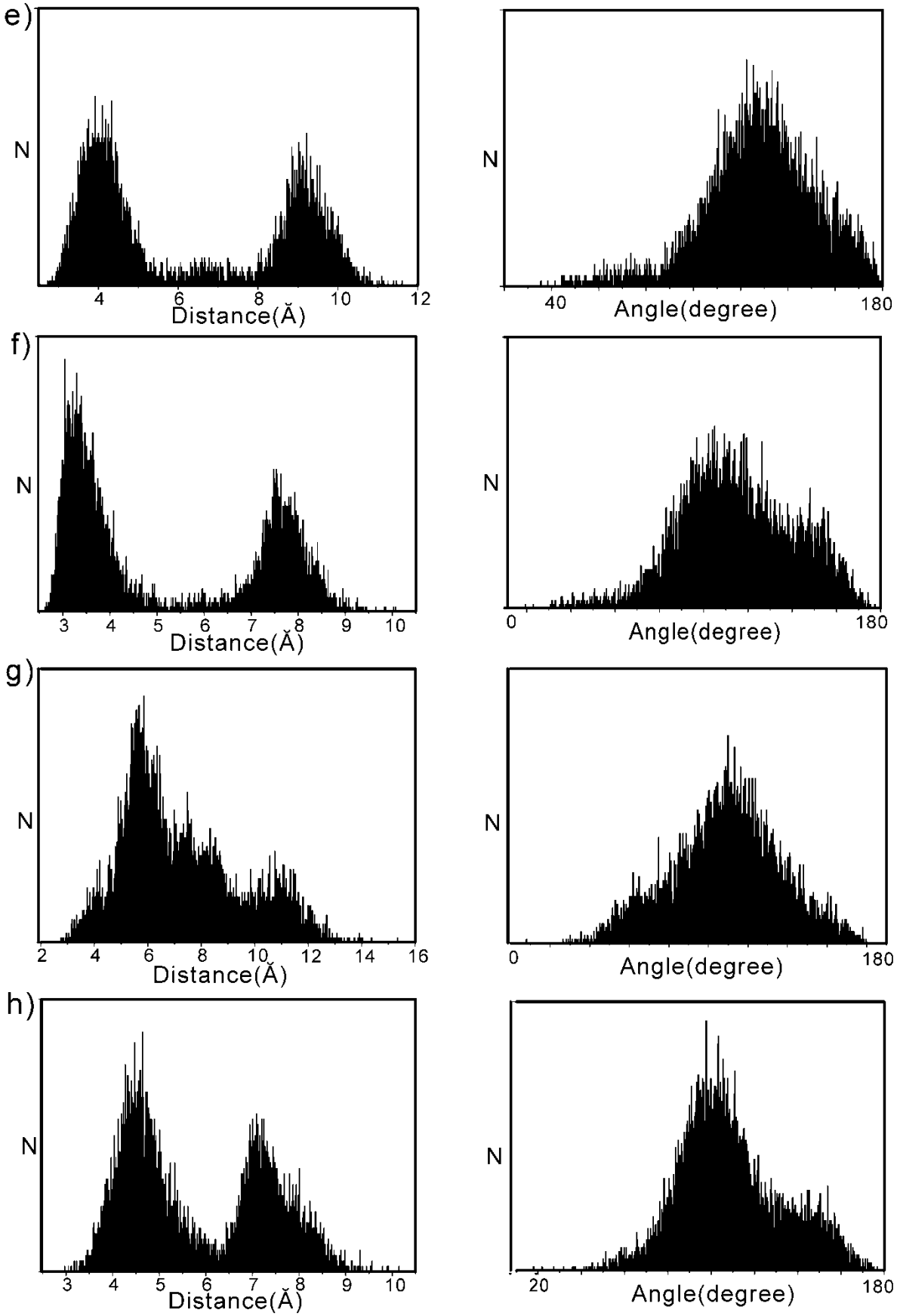
e)
N
4
6
8
10
12
Distance(Ă)
N
40
Angle(degree)
180
f)
N
3
4
5
6
7
8
9
10
Distance(Ă)
N
0
Angle(degree)
180
g)
N
2
4
6
8
10
12
14
16
Distance(Ă)
N
0
Angle(degree)
180
h)
N
3
4
5
6
7
8
9
10
Distance(Ă)
N
20
Angle(degree)
180

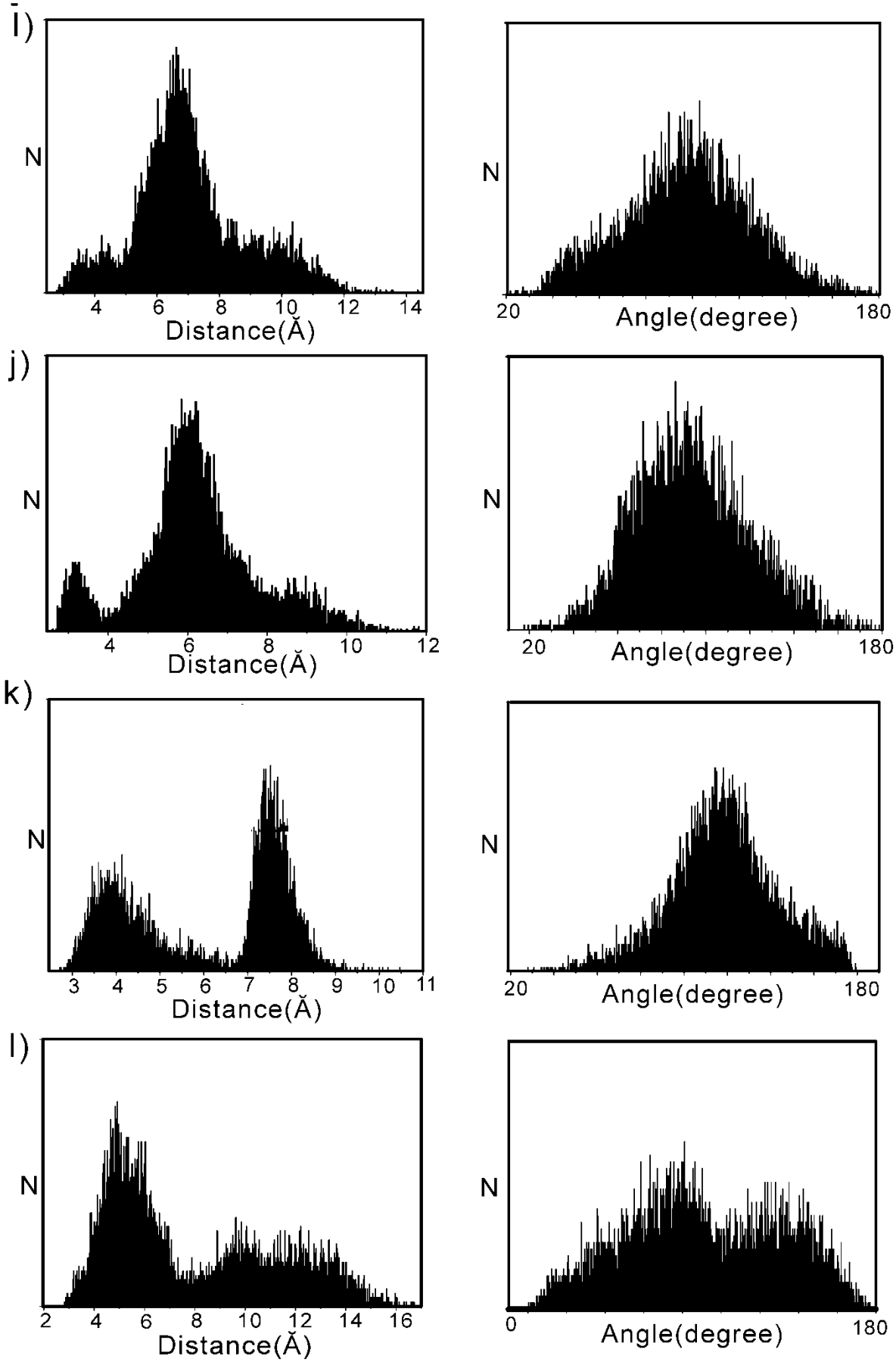
i)
N
4 6 8 10 12 14
Distance(Å)
N
20
Angle(degree)
180
j)
N
4 6 8 10 12
Distance(Å)
N
20
Angle(degree)
180
k)
N
3 4 5 6 7 8 9 10 11
Distance(Å)
N
20
Angle(degree)
180
l)
N
2 4 6 8 10 12 14 16
Distance(Å)
N
0
Angle(degree)
180

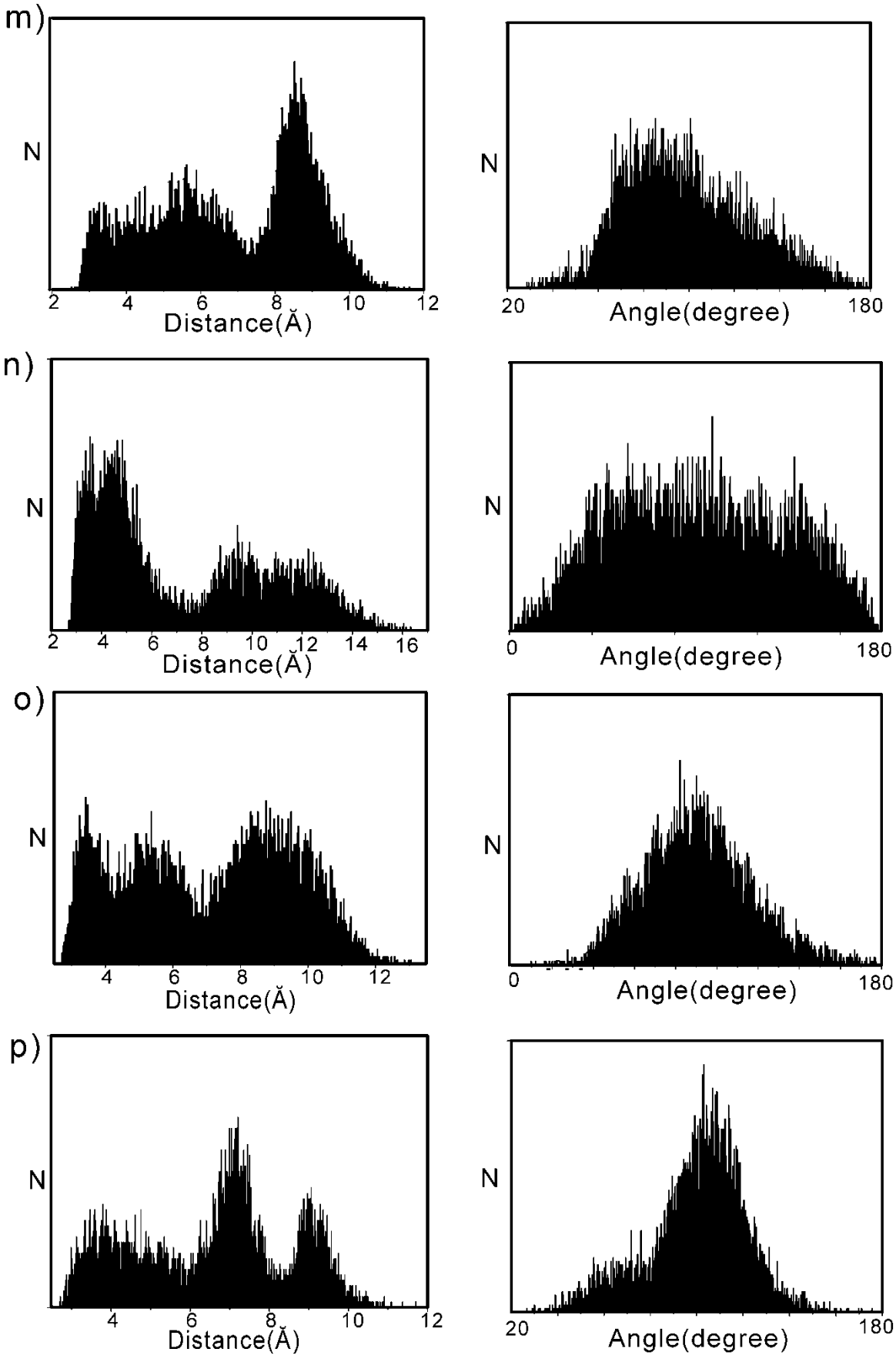
m)
N
2
4
6
8
10
12
Distance(Ă)
N
20
Angle(degree)
180
n)
N
2
4
6
8
10
12
14
16
Distance(Ă)
N
0
Angle(degree)
180
o)
N
4
6
8
10
12
Distance(Ă)
N
0
Angle(degree)
180
p)
N
4
6
8
10
12
Distance(Ă)
N
20
Angle(degree)
180

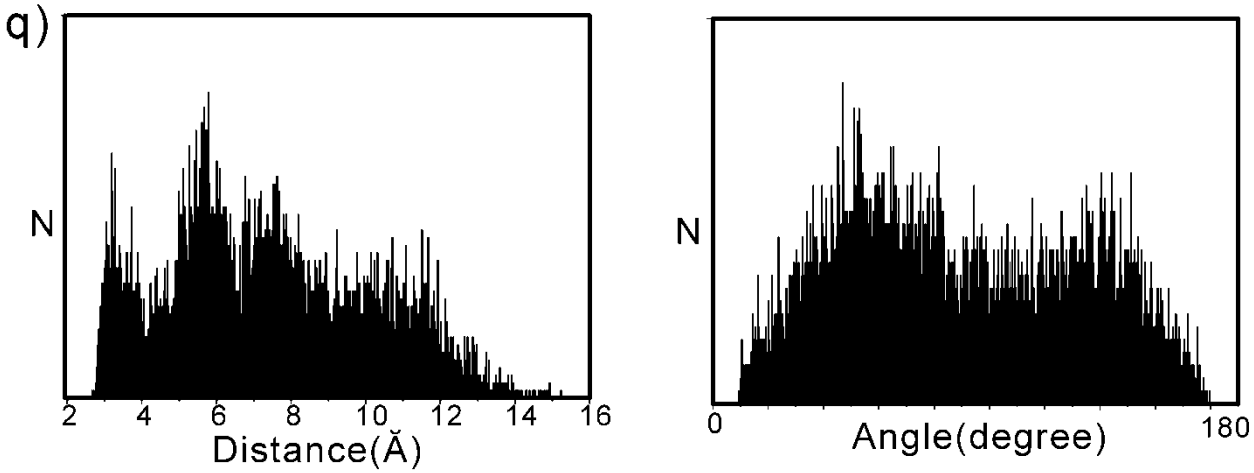

Figure S4. Distance (left) and angle (right) distributions obtained from MD simulations performed on the (Lg + 21F-SA)$^{7-}$ ion. The deprotonated residues are: Asp^{11}, Asp^{28}, Asp^{85}, Asp^{129}, Glu^{51}, Glu^{112}, Glu^{127}. (a) F^{7}/Gln^{120} H_2N (side chain), (b) F^{8}/Gln^{120} H_2N (side chain), (c) F^{9}/Gln^{120} H_2N (side chain), (d) F^{10}/Asn^{90} H_2N (side chain), (e) F^{11}/Asn^{90} H_2N (side chain), (f) F^{14}/Asn^{90} H_2N (side chain), (g) F^{14}/Asn^{88} H_2N (side chain), (h) F^{15}/Asn^{90} H_2N (side chain), (i) F^{15}/Asn^{88} H_2N (side chain), (j) F^{17}/Asn^{88} H_2N (side chain), (k) F^{18}/Asn^{90} H_2N (side chain), (l) F^{18}/Lys^{69} H_2N (side chain), (m) F^{19}/Asn^{88} H_2N (side chain), (n) F^{19}/Lys^{69} H_2N (side chain), (o) F^{21}/Asn^{88} H_2N (side chain), (p) F^{21}/Asn^{90} H_2N (side chain), (q) F^{21}/Lys^{69} H_2N (side chain). The fluorine numbering scheme is the same shown in Figure S3a.

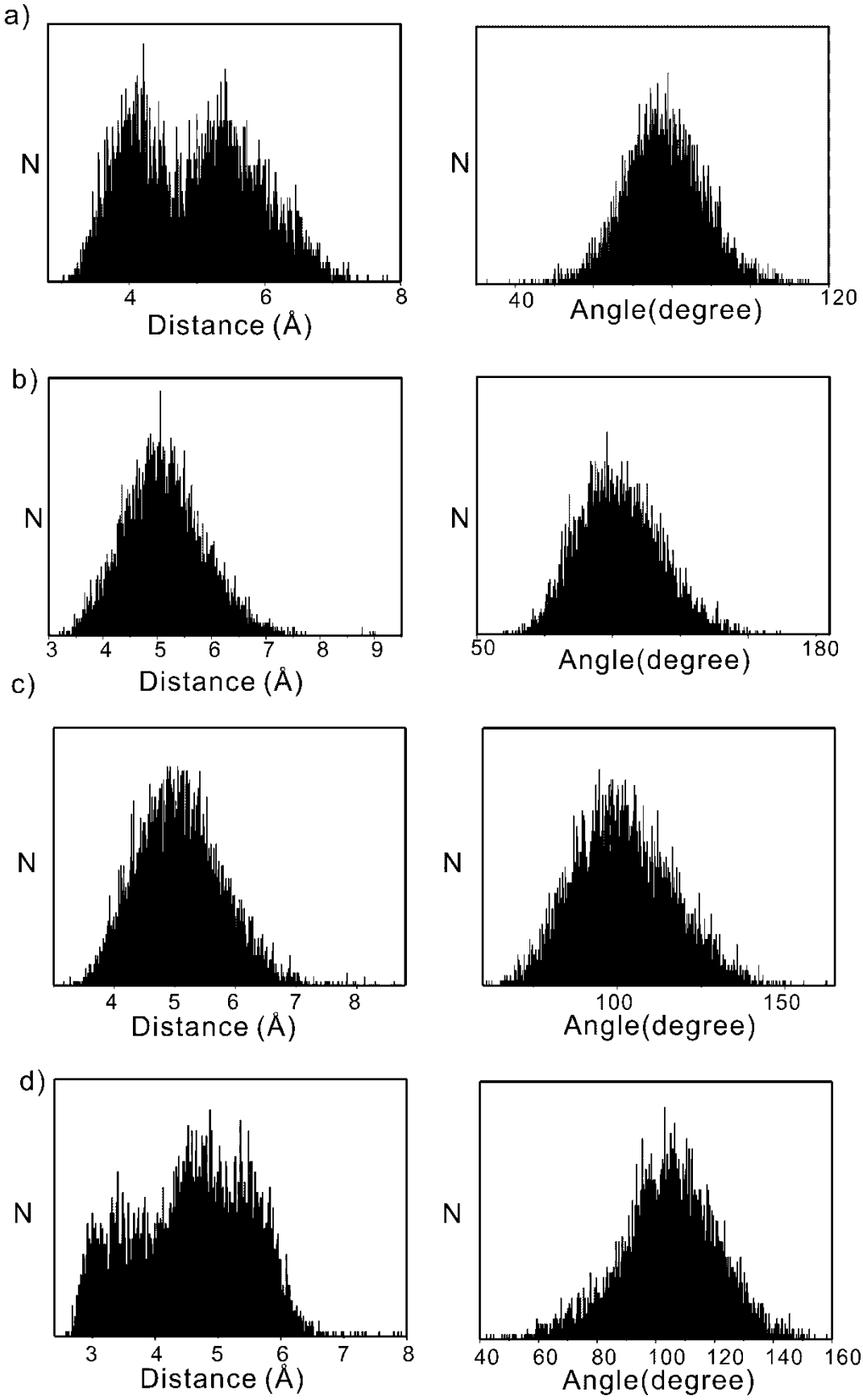
a)
N
4
6
8
Distance (Å)
N
40
120
Angle(degree)
b)
N
3
4
5
6
7
8
9
Distance (Å)
N
50
180
Angle(degree)
c)
N
4
5
6
7
8
Distance (Å)
N
100
150
Angle(degree)
d)
N
3
4
5
6
7
8
Distance (Å)
N
40
60
80
100
120
140
160
Angle(degree)

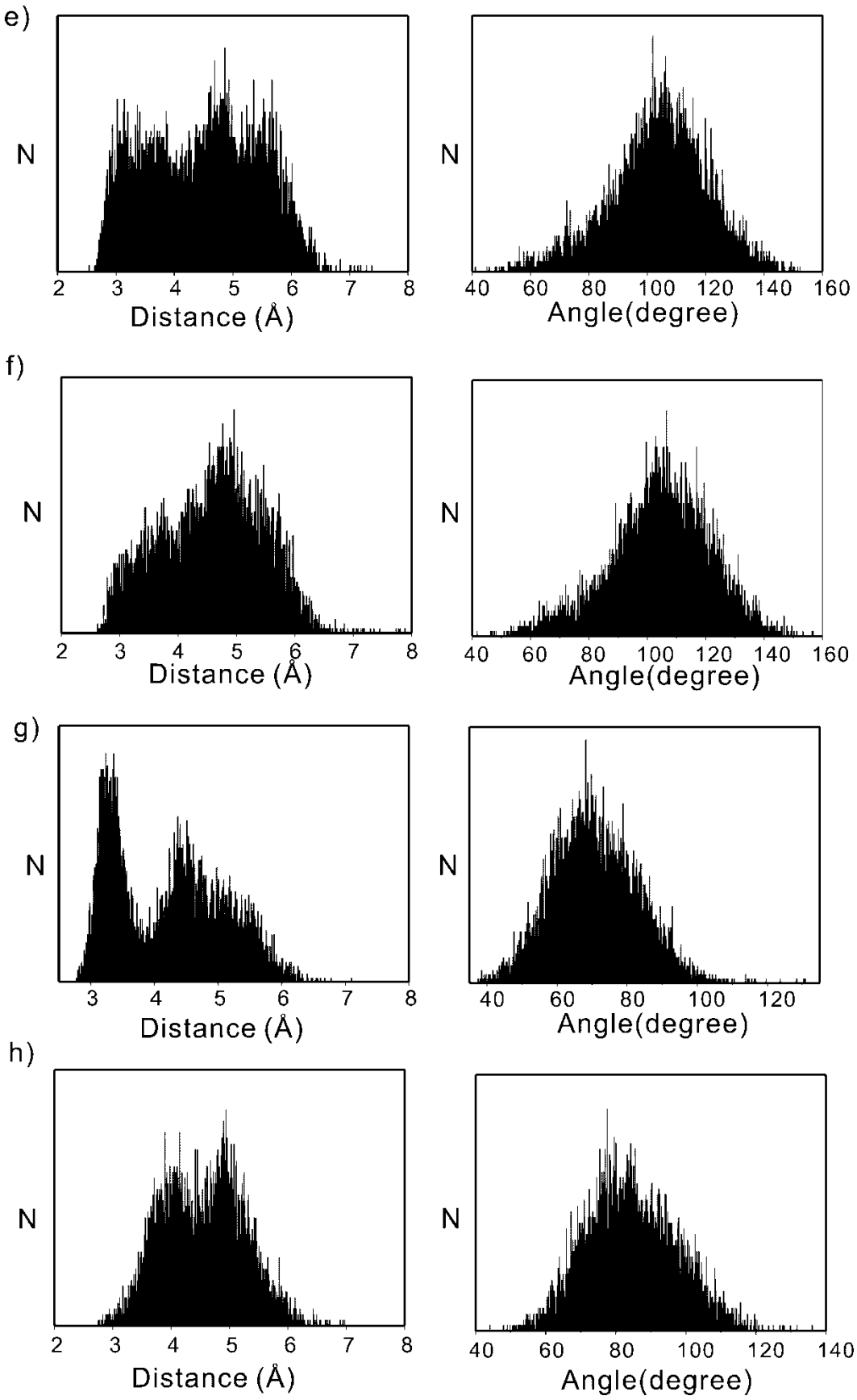
e)
N
2 3 4 5 6 7 8
Distance (Å)
N
40 60 80 100 120 140 160
Angle(degree)
f)
N
2 3 4 5 6 7 8
Distance (Å)
N
40 60 80 100 120 140 160
Angle(degree)
g)
N
3 4 5 6 7 8
Distance (Å)
N
40 60 80 100 120
Angle(degree)
h)
N
2 3 4 5 6 7 8
Distance (Å)
N
40 60 80 100 120 140
Angle(degree)

Figure S5. Distance (left) and angle (right) distributions obtained from MD simulations performed on the $(Lg + 13F\text{-}SA)^{7-}$ ion. The deprotonated residues are: Asp^{11}, Asp^{28}, Asp^{85}, Asp^{129}, Glu^{51}, Glu^{112}, Glu^{127}. (a) F^4/Leu^{93} HN (amide N), (b) F^2/Phe^{82} HN (amide N), (c) F^3/Phe^{82} HN (amide N), (d) F^1/Val^{94} HN (amide N), (e) F^2/Val^{94} HN (amide N), (f) F^3/Val^{94} HN (amide N), (g) F^4/Val^{94} HN (amide N) and (h) F^5/Val^{94} HN (amide N). The fluorine numbering scheme is the same as shown in Figure S3b.

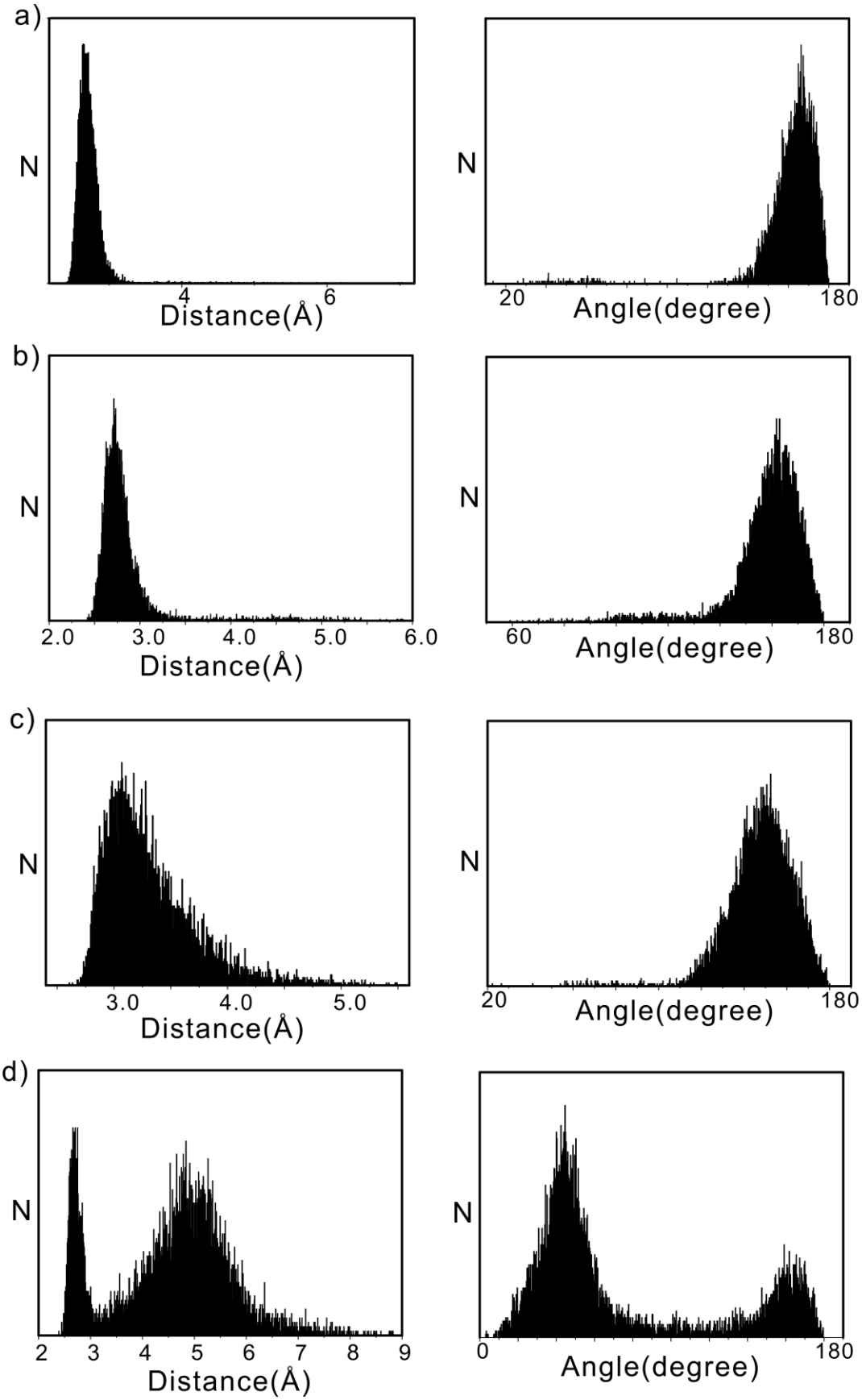
a)
N
4
6
Distance(Å)
N
20
180
Angle(degree)
b)
N
2.0
3.0
4.0
5.0
6.0
Distance(Å)
N
60
180
Angle(degree)
c)
N
3.0
4.0
5.0
Distance(Å)
N
20
180
Angle(degree)
d)
N
2
3
4
5
6
7
8
9
Distance(Å)
N
0
180
Angle(degree)

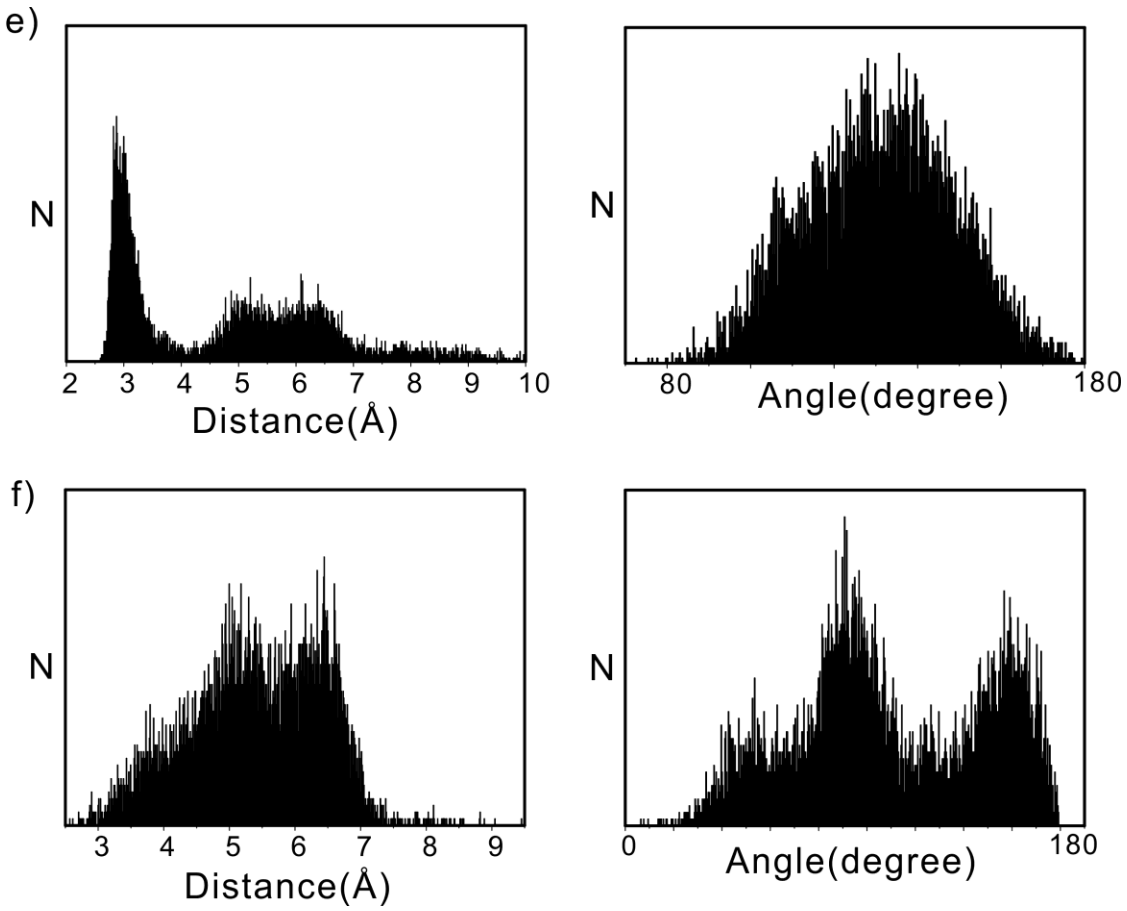

Figure S6. Distance (left) and angle (right) distributions for H-bonds obtained from MD simulations performed on the (a-c) (Lg + 13F-SA)$^{7-}$ ion and (d-f) (Lg + 21F-SA)$^{7-}$ ion. The deprotonated residues are: Asp^{11}, Asp^{28}, Asp^{85}, Asp^{129}, Glu^{51}, Glu^{112}, Glu^{127}. (a) 13F-SA C=O/Glu^{62} OH side chain (hydrogen donor), (b) 13F-SA –OH/Asn^{88} O side chain (hydrogen acceptor), (c) 13F-SA C=O/Lys^{60} H_2N, side chain (hydrogen donor), (d) 21F-SA C=O/Glu^{62} OH side chain (hydrogen donor), (e) 21F-SA C=O/Asn^{63} amide NH (hydrogen donor), and (f) 21F-SA -OH/Ser^{36} amide O (hydrogen acceptor).